

Cation– π -Anion Interaction in Alkali Ion–Benzene–Halogen Ion Clusters[†]Margarita Albertí,^{*,‡} Antonio Aguilar,[‡] and Fernando Pirani[§]*IQTCUB, Departament de Química Física, Universitat de Barcelona, Barcelona, Spain, and Dipartimento di Chimica, Università di Perugia, Perugia, Italy**Received: May 25, 2009; Revised Manuscript Received: June 29, 2009*

The present investigation on some ternary M^+ –benzene– X^- aggregates follows previous studies concerning the binary, M^+ –benzene ($M = \text{Li, Na, K, Rb, Cs}$) and X^- –benzene ($X = \text{F, Cl, Br, I}$), systems. A semimempirical model describing the intermolecular potential energy, formulated as a combination of few leading effective components, is here extended and applied to investigate more complex systems. The balancing of size repulsion with induction and dispersion attraction is described as a combination of ion–bond interactions and an electrostatic component, rationalized on the basis of the benzene quadrupole moment, is also included. For M^+ –benzene– X^- aggregates, the simultaneous presence of a cation and an anion close to the π system originates a strong Coulombic attraction and nonadditivity effects of the induction energy, which are carefully considered and explicitly included to obtain a proper analytical functional representation of the ternary compound. The proposed semiempirical methodology, providing the whole potential energy surface in a convenient analytical form, is useful to predict the main features of stable and unstable configurations, saddle points, and energy barriers, allowing for investigation of their influence on molecular dynamics simulations.

1. Introduction

It is well-known that a complete investigation of static and dynamic properties of molecular aggregates requires an accurate description of the whole potential energy surface (PES). However, for several systems, accurate ab initio calculations are too computer-time demanding to investigate the whole configuration space and, in general, only the most stable geometries are well characterized. These studies provide accurate but partial information on the system, which is often insufficient to investigate its dynamic behavior. In these cases, semiempirical methods are of fundamental importance to describe the whole interaction, adopting analytical functional representations of the PES, usually expressed as a combination of a limited number of terms having, as much as possible, a physical meaning.

Noncovalent intermolecular interactions,¹ usually much weaker than typical covalent components, affect the structure of many molecular aggregates and control the dynamics of several elementary processes occurring between closed shell species, playing an important role in chemistry, physics, and biology (see for instance refs 2–20). Particular attention has been paid to molecular aggregates involving organic molecules,^{21–33} for which noncovalent intermolecular interactions control basic phenomena such as the formation of weak hydrogen bonds,^{2,21} the competitive solvation of ions by different partners,^{21,22,34} and molecular recognition and selection processes.^{23,24,35} The study of these systems can be very useful also in rational material design, construction of new materials with defined properties, etc.^{36–38} In particular, noncovalent interactions between cations and aromatic molecules (called cation– π interactions) are of great importance in several systems as, for instance, cation receptors and biomolecules.^{32,39} Recently, the possible role of anion– π interactions in molecular anion recognition, has been also emphasized.⁴⁰ However, while the interaction of positive

ions with π electron cloud systems have been thoroughly investigated,^{24,41–44} anion–aromatic systems have received less attention. This, probably stems out of the intuitive mind that the charge distribution, associated with the π electronic cloud of the aromatic ring, stabilizes cation clusters (because of the attractive nature of the related electrostatic interaction) while destabilizes the anion ones (because of the repulsive nature of the involved electrostatic interaction). Moreover, anion– π interactions are strongly affected by dispersion energies that, to be accurately described by ab initio calculations, require the use of large basis sets and the proper inclusion of electron correlation.⁴⁵ Nevertheless, despite these difficulties, the important role that anion– π interactions can play in several fields, as in the design of new receptors stereoselectively binding anionic guests,^{46,47} in organic synthesis,⁴⁸ in solvation in heterogeneous media,⁴⁹ as well as in anion recognition processes,^{50,51} has fueled a revisitation of this topic.^{52–54}

Cation– π and anion– π interactions are typically governed by the combination of various components of noncovalent intermolecular interaction and stem from a delicate balance of competing and cooperative effects. The accurate assessment of the relative role played by the various components, like the electrostatic (of either attractive or repulsive nature), the exchange or size (of repulsive nature), and the induction, dispersion, and charge transfer (of attractive nature) is a difficult task. For this reason, semiempirical methods, which express total intermolecular interaction as a combination of a few “effective” terms representative of the leading interaction components, but also indirectly accounting for less important effects, become important tools to describe the whole PES. Intermolecular energy is often described using only two terms called “nonelectrostatic” and “electrostatic”, which also include some less important contributions, thus indirectly accounting for their incomplete separability. In particular, the nonelectrostatic term usually represents the balancing of dispersion-induction attraction and size repulsion effects.

[†] Part of the “Vincenzo Aquilanti Festschrift”.

* Corresponding author. E-mail: m.alberti@ub.edu.

[‡] Universitat de Barcelona.

[§] Università di Perugia.

In the last years, some of us developed a semiempirical model for (atom) ion–molecule systems,⁵⁵ which express the nonelectrostatic component as a sum of (atom)ion–bond interaction contributions, each one formulated by means of an improved Lennard-Jones potential (ILJ) function.⁵⁶ The involved potential parameters were predicted by exploiting the concept of bond polarizability additivity to represent both the molecular repulsion and the molecular attraction.⁵⁷ The model was applied to investigate some clusters containing ions and benzene (bz) and the electrostatic term was formulated as a sum of Coulombic contributions providing asymptotically the ion–benzene quadrupole interaction.⁵⁸ The validity of the model was tested by carrying out extensive ab initio calculations for both alkali cation (M⁺)–bz^{43,59} and halogen ion (X[−])–bz, aggregates.^{60,61} The proposed analytical function to represent the whole PES has been proved to be very useful in MD calculations.^{58,62–66}

The investigation of M⁺–bz–X[−] ternary aggregates, by extending the methodology applied to binary compounds, has been motivated by both the good results obtained for ion–bz systems and the assessment of competing effects between interaction forces of different nature. Although the most stable gas phase structure corresponds to the bz–M⁺–X[−] arrangement, our interest deals mainly with the study of M⁺–bz–X[−] structures⁴⁵ to obtain, first, direct information on the cation– π –anion interaction and, accordingly, on the full PES. In particular, in biological systems, the assessment of the role of noncovalent interactions in the presence of competing forces is an interesting research field.⁶⁷ Moreover, ternary systems are involved in most of the intermolecular interactions, for instance the adsorption and distribution of ions at the interface of water and crown ethers,^{68–70} and the relative arrangement of ions at the vapor/liquid interface of atmospheric particle surfaces.^{71,72} In particular, systems containing ions of different sign can play a crucial role in some cation channels. For instance, in the ammonia channel, the presence of an anion (the negatively charged amino acid, Asp¹⁶⁰) plays a key role when the ammonium cation interacts with some of the amino acid residues.⁴⁵ In fact, the electrostatic interaction between anions and cations facilitates the cation– π interactions. However, despite the importance of investigating ternary compounds, it must be indicated here that, up to date, theoretical investigations have focused their attention mainly on binary complexes.

In respect to the related binary compounds, the presence of a second ion in M⁺–bz–X[−] originates important induction effects, because of its nonadditivity behavior. In fact, the induction energy is strongly enhanced when ions of different sign are placed on opposite sides of the aromatic ring, while it tends to zero when anion and cation are placed on the same side and approximately at the same distance from the aromatic ring. This indicates that to extend our semiempirical method to investigate M⁺–bz–X[−] aggregates, the induction energy must be properly assessed.

The paper is structured as follows: in section 2 we outline the formulation of the semiempirical PES, proposing a treatment of the induction energy, and in section 3 the results are presented and discussed. Concluding remarks are given in section 4.

2. Semiempirical Potential Energy Surface

The total intermolecular interaction energy, V , for M⁺–bz–X[−] aggregates is decomposed as

$$V = V_{M^+-bz} + V_{X^--bz} + V_{M^+-X^-} + V'_{ind} \quad (1)$$

V_{M^+-bz} and V_{X^--bz} , accounting for the whole cation–bz and anion–bz interactions, respectively, are expressed by a sum of electrostatic, V_{el} , and nonelectrostatic, V_{nel} , terms.^{55,58,59,62–64,73} $V_{M^+-X^-}$, representing the ion pair interaction, is given as an unique effective contribution including both, V_{el} and V_{nel} . Finally, V'_{ind} accounts for the nonadditivity behavior of induction effects (see below).

More in detail, the V_{nel} component used to describe V_{M^+-bz} and V_{X^--bz} is constructed by applying the concept of molecular bond polarizability additivity and is expressed as a sum of ion–bond interaction contributions (6 M⁺–CC and 6 M⁺–CH for M⁺–bz; 6 X[−]–CC, 6 X[−]–CH for X[−]–bz). This formulation, as emphasized previously,^{59–61} allows its generalization to systems of increasing complexity.

Each ion–bond contribution is represented by means of the ILJ function,^{55,56}

$$V_{ILJ}(r, \gamma) = \varepsilon(\gamma) \left[\frac{m}{n(r, \gamma) - m} \left(\frac{r_0(\gamma)}{r} \right)^{n(r, \gamma)} - \frac{n(r, \gamma)}{n(r, \gamma) - m} \left(\frac{r_0(\gamma)}{r} \right)^m \right] \quad (2)$$

where r represents the distance of a given ion from the center of a bond and γ is the angle that the \mathbf{r} vector forms with the bond. The m parameter is taken equal to 4, the typical value for ion–neutral interactions. The well depth ε and the equilibrium distance r_0 are modulated through simple trigonometric formula from the corresponding perpendicular (ε_{\perp} , $r_{0\perp}$) and parallel (ε_{\parallel} , $r_{0\parallel}$) values (see for instance ref 58). This allows us to take into account the variation of the well depth and the equilibrium distance for different approaches of an ion to a particular bond ($\varepsilon(\gamma)$ and $r_0(\gamma)$). The first term in eq 2 (positive) represents the size–repulsion contribution arising from each ion–bond pair, while the second one (negative) provides dispersion plus induction effective attraction ascribed to the same pair. The $n(r, \gamma)$ exponent, defining the falloff of the ion–bond repulsion is expressed as

$$n(r, \gamma) = \beta + 4.0 \left(\frac{r}{r_0(\gamma)} \right)^2 \quad (3)$$

where β is an adjustable parameter related to the hardness of the interacting partners.^{55,56} Taking into account the higher polarizability of X[−] ions with respect to that of the corresponding isoelectronic positive alkali ions, the value of β used to describe anion–bz interactions has been assumed to be lower than for the cation–bz ones. For all ion–bond pairs the perpendicular and parallel values of ε and r_0 have been predicted using the ion polarizability as well as polarizability and effective polarizability tensor components of the C–C and C–H benzene bonds.^{55,57,58,65} All parameters defining the ion–bond interactions are given in Table 1.

It is of interest to note that the popular Lennard-Jones potential, obtained by fixing $n = \text{constant}$ in eq 3 and still extensively used in molecular dynamics (MD) calculations, is too repulsive at short distances and too attractive at long-range. Most of these inadequacies are removed when the ILJ function is conveniently parametrized. In fact, an extensive analysis of some ionic and neutral systems confirmed that actually ILJ can cover a wide range of phenomenology.⁵⁶

The electrostatic component of the interaction, V_{el} , has been evaluated as in our previous studies of the binary ion–bz

TABLE 1: Perpendicular and Parallel Components of the Well Depth (ε_{\perp} , ε_{\parallel}) and of the Equilibrium Distances ($r_{0\perp}$, $r_{0\parallel}$) for the Different Ion–Bond Pairs and β Parameter

ion–bond	$\varepsilon_{\perp}/\text{meV}$	$\varepsilon_{\parallel}/\text{meV}$	$r_{0\perp}/\text{Å}$	$r_{0\parallel}/\text{Å}$	β
Na ⁺ –CC	33.01	102.20	2.848	3.149	8.5
Na ⁺ –CH	62.15	62.73	2.601	2.808	8.5
K ⁺ –CC	22.95	75.77	3.266	3.547	8.5
K ⁺ –CH	39.97	42.70	3.044	3.240	8.5
Rb ⁺ –CC	20.52	69.77	3.435	3.705	8.5
Rb ⁺ –CH	34.58	37.58	3.225	3.417	8.5
Cs ⁺ –CC	18.20	64.11	3.638	3.894	8.5
Cs ⁺ –CH	29.42	32.57	3.445	3.632	8.5
Cl [−] –CC	16.37	59.64	3.832	4.073	7.0
Cl [−] –CH	25.48	28.60	3.655	3.839	7.0
Br [−] –CC	15.20	56.73	3.972	4.202	7.0
Br [−] –CH	23.06	26.10	3.808	3.990	7.0
I [−] –CC	13.76	52.96	4.166	4.380	7.0
I [−] –CH	20.22	23.18	4.018	4.198	7.0

TABLE 2: Well Depth (ε), Equilibrium Distance (r_0), and β Parameter Defining the M⁺–X[−] Interactions

M ⁺ –X [−]	ε/meV	$r_0/\text{Å}$	β
Na ⁺ –Cl [−]	5740	2.32	8.0
K ⁺ –Cl [−]	5160	2.65	8.0
Rb ⁺ –Cl [−]	5000	2.78	8.0
Cs ⁺ –Cl [−]	4850	2.95	8.0
Na ⁺ –Br [−]	5540	2.47	8.0
K ⁺ –Br [−]	5030	2.80	8.0
Rb ⁺ –Br [−]	4900	2.93	8.0
Cs ⁺ –Br [−]	4790	3.09	8.0
Na ⁺ –I [−]	5330	2.68	8.0
K ⁺ –I [−]	4910	3.00	8.0
Rb ⁺ –I [−]	4820	3.13	8.0
Cs ⁺ –I [−]	4750	3.28	8.0

clusters, considering the ion charge and an ensemble of 18 charge points distributed on the benzene molecule frame (6 placed on the H atoms and the remaining 12 at a fixed distances from C atoms on both sides of the aromatic ring). Such distribution has been chosen from the consideration that, asymptotically, V_{el} must correspond to the ion quadrupole interaction.⁵⁸ This leads to a charge of +0.09245 au on each H atom and to two negative charges of −0.04623 au separated by 1.905 Å on each C atom, placed on opposite sides of the benzene plane.

For M⁺–X[−], all involved interaction components exhibit a single radial dependence. Therefore, $V_{\text{M}^+-\text{X}^-}$ has been represented by eq 2, after removing the angular dependence (ε and r_0 no longer depend on γ). In this case, the parameters of the effective potential function for $V_{\text{M}^+-\text{X}^-}$ have been chosen to account directly for the effective combination of V_{el} and V_{nel} . Consequently, the first term (positive) of eq 2 represents the size-repulsion contribution arising from the interaction between the two ions, while the second term (negative) provides the effective attraction arising from electrostatic, dispersion and induction effects. Accordingly, with this representation m is taken equal to 1, since the charge–charge electrostatic contribution dominates the asymptotic attraction. All parameters are given in Table 2.

The induction energy in M⁺–bz–X[−] requires a more careful treatment. In fact, part of its full contribution is implicitly enclosed, by means of effective ion–bond interactions, in the formulation of the binary compounds interaction. Accordingly, V'_{ind} in eq 1 does not represent the whole induction energy, but only the fraction accounting for nonadditivity behavior arising because of the simultaneous presence of two ions in the aggregates (the induction energy excess or lack in respect to

TABLE 3: Parallel, α_{\parallel} , and Perpendicular, α_{\perp} , Components of the CC and CH Bond Polarizabilities

	$\alpha_{\parallel}/\text{Å}^3$	$\alpha_{\perp}/\text{Å}^3$
CC	1.78	0.38
CH	0.67	0.49

the additivity of binary contributions). Specifically, as indicated above, the presence of a second ion introduces important variations of the induction energy, whose value depends on the geometry of the ternary compound. This approach ensures an accurate description of the binary compounds when the ternary dissociates, predicting the correct potential energy for both M⁺–bz and X[−]–bz systems (this is of fundamental importance in MD simulations).

V'_{ind} in eq 1 can be formulated by first considering full induction effects, V_{ind} , and then removing the contributions enclosed yet in the binary compounds. Therefore, V_{ind} accounts for the full global effect that ion 1 and 2 create on bz ($V_{12,\text{ind}}$) plus the effects promoted by ion 1 on ion 2 and vice versa ($V_{1,\text{ind}}$ and $V_{2,\text{ind}}$, respectively),

$$V_{\text{ind}} = V_{12,\text{ind}} + V_{1,\text{ind}} + V_{2,\text{ind}} \quad (4)$$

Following the present methodology, $V_{12,\text{ind}}$ is represented as combination of parallel (\parallel) and perpendicular (\perp) components, each one defined as a sum of parallel, $V_{\parallel,\text{ind}}$, and perpendicular, $V_{\perp,\text{ind}}$, ion–bond contributions, expressed as

$$V_{\parallel,\text{ind}} = -\frac{1}{2} \left(\frac{q_1^2}{r_1^4} \cos^2 \gamma_1 + \frac{q_2^2}{r_2^4} \cos^2 \gamma_2 + 2 \frac{q_1}{r_1^2} \frac{q_2}{r_2^2} \cos \gamma_1 \cos \gamma_2 \right) \alpha_{\parallel} \quad (5)$$

$$V_{\perp,\text{ind}} = -\frac{1}{2} \left(\frac{q_1^2}{r_1^4} \sin^2 \gamma_1 + \frac{q_2^2}{r_2^4} \sin^2 \gamma_2 + 2 \frac{q_1}{r_1^2} \frac{q_2}{r_2^2} \sin \gamma_1 \sin \gamma_2 \cos \omega \right) \alpha_{\perp} \quad (6)$$

where the quantity in parentheses defines the square of the total electric field component generated by the two ions (parallel and perpendicular to each bond). In eqs 5 and 6, r_i and r_j are the distances from i and j ions to the center of a bond. As in eq 2, γ_1 and γ_2 represent the angle that a given bond forms with \mathbf{r}_i and \mathbf{r}_j vectors. α_{\parallel} and α_{\perp} are the bond polarizability components whose values are given in Table 3 (these values are the same used to estimate the potential parameters given in Table 1). In eq 6, ω is the dihedral angle that the plane defined by the ion i and the AB bond forms with that defined by j ion and the same bond. The evaluation of $V_{12,\text{ind}}$ involves 24 planes (6 i -CC, 6 i -CH, 6 j -CC, and 6 j -CH).

The remaining contributions to V_{ind} , $V_{1,\text{ind}}$ and $V_{2,\text{ind}}$, are represented as,

$$V_{1,\text{ind}} = -\frac{1}{2} \frac{q_1^2}{r_{12}^4} \alpha_2 \quad (7)$$

$$V_{2,\text{ind}} = -\frac{1}{2} \frac{q_2^2}{r_{12}^4} \alpha_1$$

where the index 1 is for the cation and the 2 for the anion. Accordingly, α_1 and α_2 are the polarizabilities of cation and ion, respectively, whose values are given in Table 4.

The three body contribution, V'_{ind} , mainly arising from nonadditivity behavior, can be isolated, as indicated above, by subtracting the induction energies of the binary compounds to V_{ind} .

Each bond contribution to V'_{ind} is given again as combination of its parallel, $V'_{\text{ll,ind}}$ and perpendicular, $V'_{\text{⊥,ind}}$, components,

$$V'_{\text{ll,ind}} = -\frac{q_1 q_2}{r_1^2 r_2^2} \cos \gamma_1 \cos \gamma_2 \alpha_{\parallel} \quad (8)$$

$$V'_{\text{⊥,ind}} = -\frac{q_1 q_2}{r_1^2 r_2^2} \sin \gamma_1 \sin \gamma_2 \cos \omega \alpha_{\perp} \quad (9)$$

Following the present formulation for all interaction contributions the total potential energy, V , is expressed as

$$V = \sum_{i=1}^6 V_{\text{M}^+-\text{(CC)}_i} + \sum_{i=1}^6 V_{\text{M}^+-\text{(CH)}_i} + \sum_{i=1}^6 V_{\text{X}^--\text{(CC)}_i} + \sum_{i=1}^6 V_{\text{X}^--\text{(CH)}_i} + V_{\text{M}^+-\text{X}^-} + V_{\text{el}} + V'_{\text{ind}} \quad (10)$$

where V_{el} represents the electrostatic energy arising from M^+-bz and X^--bz interactions, calculated as previously^{58,62–65} by summing Coulombic terms according with bz charge distribution and charges of +1 au and -1 au assigned to M^+ and X^- , respectively. V_{el} do not represent the total electrostatic energy of the ternary aggregate but only a fraction, because electrostatic energy arising from the M^+-X^- interaction has been implicitly enclosed in the effective $V_{\text{M}^+-\text{X}^-}$ potential function.⁷⁴

3. Results and Discussion

The present investigation focuses on structure and energetic of $\text{M}^+-\text{bz}-\text{X}^-$ aggregates, for which an extension of the original semiempirical approach, introduced before for simpler systems, is carried out by including nonadditive induction effects. The full intermolecular potential, V (see eq 10), is given as a combination of a few leading effective interaction components, all expressed by proper functional forms whose parameters have a physical meaning. The reliability of the obtained full PES is here tested in detail by analyzing first the related binary compounds (M^+-X^- , M^+-bz , and X^--bz), obtained from $\text{M}^+-\text{bz}-\text{X}^-$ following the various dissociating channels, and second comparing some important features of ternary aggregates, in specific configurations, with ab initio results. Role and strength of three body effects are also discussed in detail.

M^+-X^- Systems. As indicated in the previous section, the interaction between M^+ and X^- to form M^+-X^- , is described by means of an effective potential function of the ILJ type,^{56,74}

TABLE 4: Ion Polarizabilities (Also Ref 74)

	Na^+	K^+	Rb^+	Cs^+	Cl^-	Br^-	I^-
$\alpha/\text{\AA}^3$	0.18	0.85	1.41	2.42	3.82	5.16	7.53

including both electrostatic and nonelectrostatic interactions. The parameters of the potential function given in Table 3 have been obtained as indicated in ref 74. In general, it has been found that the ILJ function provides a good description of the systems at long-range and at intermediate distances.⁵⁶ It must be stressed here that, because our interest in studying the $\text{M}^+-\text{bz}-\text{X}^-$ cluster arrangement, for which the internuclear distance from M^+ to X^- is much larger than the equilibrium distance for M^+-X^- systems, accurate descriptions of the M^+-X^- long-range interaction are of fundamental importance. This request is particularly stringent when the whole potential energy function is thought to be used in molecular dynamic simulations. It must be stressed here that $V_{\text{M}^+-\text{X}^-}$ functions give asymptotic charge-charge constants, $C_1 = \epsilon r_0$, which exhibit a maximum deviation from the single charge-single charge Coulombic constant ($C_1 = 14.40 \text{ eV \AA}$) of only 8%.

M^+-bz and X^--bz Systems. As can be expected from the benzene charge distribution, the binary M^+-bz and X^--bz aggregates show important differences. The alkali cations exhibit an attractive interaction with the aromatic ring and the most stable configuration is found for approaches of M^+ toward bz along C_6 symmetry axis. On the contrary, V_{el} favors approaches of X^- on the benzene plane and the most stable structure is found when X^- approaches bz on plane, perpendicularly to CC bonds (bifurcated structure).

The quality of the potential function for M^+-bz aggregates⁵⁸ was tested by carrying out high level ab initio calculations.⁵⁹ Results showed an extremely good agreement for heavier metal ions (K^+ , Rb^+ , and Cs^+) with minimal differences between the two theoretical approaches (semiempirical method and ab initio calculations) at all considered geometries. Results in reasonable good agreement were obtained for Na^+ , while some deviations were observed for Li^+ . These results suggest that chemical contributions play a minor role, at least for the heavier M^+-bz aggregates.

Semiempirical geometry and energy predictions for X^--bz have also been tested by comparing them with high level ab initio calculations.^{60,61} In general, the semiempirical predictions are in reasonable agreement with experimental and ab initio results. However, again, the best agreement is for the heavier Br^--bz and I^--bz systems, while for Cl^--bz the predictions are not far from ab initio results. Some deviations have been observed for the lightest F^--bz (possible reasons are discussed in ref 61). Taking into account the formulation of the semiempirical method, by means of simple analytical functions, and assuming that the potential effective parameters have been predicted only from basic physical properties of the involved partners, the obtained semiempirical results can be considered, in general, very good. Values of dissociation energy and equilibrium distance of ion from bz center of mass are given in Table 5 for the most stable M^+-bz ($\text{M} = \text{Na}, \text{K}, \text{Rb}, \text{Cs}$) and X^--bz ($\text{X} = \text{Cl}, \text{Br}, \text{I}$) structures.

In Figure 1, for two representative systems, K^+-bz (upper panel) and Br^--bz (lower panel), are shown the equipotential energy contours for movements of ions on the yz plane (bz is placed on the xy plane). The interaction differences between cation-bz and anion-bz are well evidenced in the figure, where the lowest energy contour is indicated and consecutive contours are spaced by 100 meV. The PES is very attractive for

TABLE 5: Dissociation Energy, D_e , and Equilibrium Distance, R_e , of the Ion from the Benzene Center of Mass, Associated to the Most Stable Configuration of Ion–bz Systems

	Na ⁺ –bz	K ⁺ –bz	Rb ⁺ –bz	Cs ⁺ –bz	Cl [−] –bz	Br [−] –bz	I [−] –bz
D_e/meV	1270	942	841	736	314	296	272
$R_e/\text{Å}$	2.25	2.65	2.82	3.02	4.87	5.00	5.19

approaches of K⁺ to benzene along the symmetry axis, while it is very repulsive for approaches of Br[−] to benzene along that axis.

It must be indicated that the PES's do not show spurious points, and being represented by simple analytical forms, they are very useful in MD simulations. In fact, the PES's for M⁺–bz and X[−]–bz have been implemented in the DL_POLY program⁷⁵ and MD calculations have been carried out for the M⁺–bz,^{58,62–64} Cl[−]–bz,⁶⁵ and I[−]–bz⁶⁶ systems solvated by Ar atoms.

Because of our interest in characterizing mainly the M⁺–bz–X[−] arrangement, energy changes on the binary compounds, as a function of the distance of X[−] from bz center of mass, r_{X^-bz} , when X[−] approaches bz along the C₆ axis have also been investigated. The corresponding energy curves are represented in Figure 2, where it can be seen that the system is very repulsive for these approaches.

Ternary M⁺–bz–X[−] System. A basic structure of such systems involves cation and anion placed along the C₆ symmetry axis but in opposite sides of the aromatic ring (this structure has been also the objective of ab initio calculations⁴⁵). A total of 12 aggregates of the M⁺–bz–X[−] type (M = Na, K, Rb, Cs; X = Cl, Br, I) have been investigated. The aggregates containing Li⁺ and F[−] have not been considered here because ab initio tests^{59,61} showed that the semiempirical method can only partially account for particular effects of these ions interacting with benzene.

For all the investigated M⁺–bz–X[−] cases, predicted values of some energy contributions, minimum potential energy and distances of cation and anion from the benzene center of mass are given in Table 6. All the predicted data appear to be in

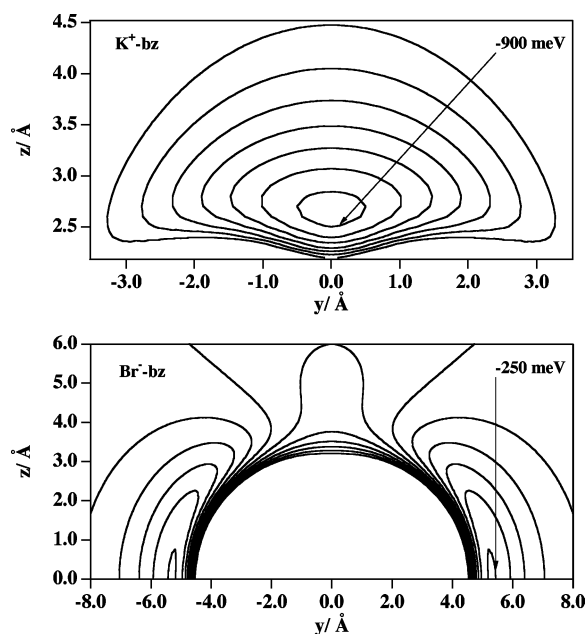


Figure 1. Equipotential energy contours for the K⁺–bz (upper panel) and for Br[−]–bz (lower panel). The benzene molecule is placed in the *xy* plane with *y* pointing along CH bonds. The lowest energy contour is indicated and consecutive contours are spaced by 100 meV.

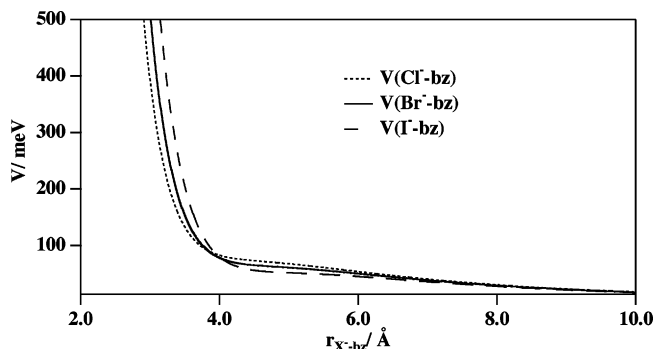


Figure 2. Total potential energy for approaches of X[−] along the C₆ symmetry axis of benzene plotted as a function of the distance r_{X^-bz} .

reasonable agreement with available ab initio results (calculated at the second order Moller-Pleset level of theory using the 6-31+G* basis set).⁴⁵ Ab initio energies and intermolecular distances are also given in Table 6, for comparison.

From the first column of Table 6 it can be seen that those aggregates containing the same cation but different anions have similar energies. On the contrary, for a given anion, the total energy increases (less negative) with the cation mass. Such trends can be appreciated in Figure 3 where total potential energies, calculated at the equilibrium of the investigated M⁺–bz–X[−] structures, are represented vs ion polarizability, which has been chosen as a property related with the size of the ions.⁷⁴ The upper panel of Figure 3 shows, for any selected cation, the trend of the potential energy when different anions (having different polarizability values) are considered, while the lower panel of the same figure reports, for any given anion, the potential energy as a function of cation polarizability. The figure remarks that the M⁺–bz–X[−] compounds containing the same cation have approximately the same potential energy, independently of the anion. These observations are in qualitative agreement with the ab initio calculations of Kim et al.⁴⁵ (concerning Na⁺–bz–X[−] and K⁺–bz–X[−] (X = Cl, Br) systems), whose results show small potential energy differences when Cl is substituted by Br (less than 1 kcal mol^{−1}). However, it must be observed that in ref 45 the lowest energy value is obtained for the lightest aggregate, while our potential model predicts the opposite behavior. Concerning the M⁺–bz–X[−] aggregates containing the same anion (see the lower panel of Figure 3), the potential energy increases as a function of cation size also agree with ab initio results.⁴⁵ As can be seen, in general, semiempirical calculations predict stabler clusters than the ab initio results and, concerning the equilibrium distances, the semiempirical method predicts higher M⁺–bz distances (r_{M^+bz}), while lower values of the X[−]–bz distances (r_{X^-bz}) are obtained. In all cases, however, the difference between semiempirical and ab initio energy results is about 10%, with smaller differences found for equilibrium distances. Some of the possible reasons for these discrepancies are, on one hand, the rigidity of the benzene molecule maintained along dynamical simulations and, on the other hand, the charge transfer effects, which do not take into account the semiempirical method. The representation of the electrostatic potential through a fixed point charge model can affect geometry and energy results. In fact, for the binary X[−]–bz systems, it has been proved⁶¹ that the electrostatic component fails to reproduce electrostatic energies at short distances. It has been found that the discrepancy in the electrostatic contribution, in the context of the overall potential has consequences only for the lighter anions (F[−] and to a lesser extent Cl[−]). On the contrary, for M⁺–bz systems a good

TABLE 6: Total Interaction Energy, $V_{M^+-bz-X^-}$, and Different Contributions: Cation–Anion, $V_{M^+-X^-}$, Cation–Benzene, V_{M^+-bz} , Anion–Benzene, V_{X^--bz} , and Three-Body Induction, V'_{ind} ^a

	$V_{M^+-bz-X^-}$	$V_{M^+-X^-}$	V_{M^+-bz}	V_{X^--bz}	V'_{ind}	r_{M^+-bz}	r_{X^--bz}
$Na^+-bz-Cl^-$	-3876 (-3680)	-2575 (-2790)	-1244 (-933)	301 (297)	-358 (-250)	2.154 (2.27)	3.200 (3.04)
$Na^+-bz-Br^-$	-3902 (-3652)	-2602 (-2731)	-1244 (-941)	292 (246)	-348 (-228)	2.154 (2.28)	3.303 (3.19)
Na^+-bz-I^-	-3953	-2657	-1244	283	-335	2.154	3.442
$K^+-bz-Cl^-$	-3419 (-3131)	-2472 (-2534)	-909 (-657)	283 (272)	-322 (-213)	2.516 (2.73)	3.231 (3.08)
$K^+-bz-Br^-$	-3453 (-3109)	-2505 (-2481)	-909 (-658)	273 (226)	-312 (-196)	2.516 (2.74)	3.335 (3.22)
K^+-bz-I^-	-3509	-2566	-909	264	-299	2.516	3.474
$Rb^+-bz-Cl^-$	-3281	-2447	-804	277	-307	2.655	3.243
$Rb^+-bz-Br^-$	-3322	-2489	-804	268	-297	2.665	3.346
Rb^+-bz-I^-	-3392	-2563	-804	259	-284	2.664	3.485
$Cs^+-bz-Cl^-$	-3156	-2444	-695	271	-289	2.844	3.253
$Cs^+-bz-Br^-$	-3203	-2491	-695	262	-279	2.844	3.356
Cs^+-bz-I^-	-3278	-2570	-695	253	-267	2.843	3.495

^a Distance of the cation and the anion from the center of mass of benzene: r_{M^+-bz} and r_{X^--bz} . The energies are given in meV and the distances in Å. Ab initio results⁴⁵ are given in parentheses.

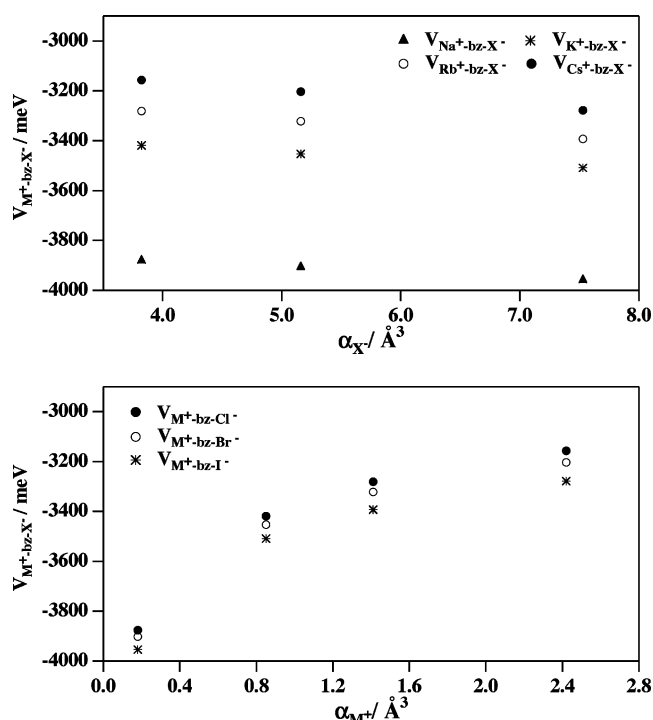


Figure 3. Total potential energy for the M^+-bz-X^- systems as a function of the ion polarizability (see text).

agreement has been found in the electrostatic contribution derived from the ab initio and semiempirical methods.⁵⁹ From Table 6 it can be seen that the higher energy differences correspond to M^+-bz contributions. This was also observed from the ab initio test performed for the binary M^+-bz systems.⁵⁹ However, it must be indicated that the ab initio results of ref 59 for K^+-bz are in better agreement with semiempirical values than the corresponding results of ref 45. This can probably be due to the different basis sets used in both ab initio calculations.

Bearing in mind that ternary aggregates have been described adopting the same values of the potential parameters used for binary compounds, without any modification, the semiempirical predictions can be considered to be very good. Moreover, it must be stressed that no refinements of β (see eq 3) have been made. Actually, the same value has been used for all members

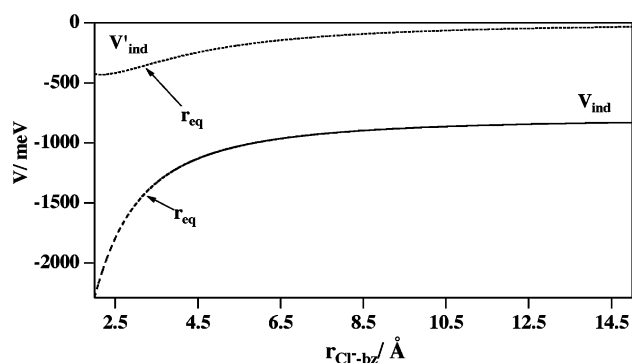


Figure 4. Total induction energy, V_{ind} , and three body contribution, V'_{ind} , for the $Na^+-bz-Cl^-$ aggregate as a function of the distance r_{Cl^-bz} taken along the C_6 symmetry axis of benzene. The r_{Cl^-bz} equilibrium distance, r_{eq} is indicated.

of the same family (i.e., 8.5 for any M^+-bond pair, 7.0 for any X^--bond pair and 8.0 for the binary M^+-X^- compounds); however, it can be expected that further refinements of β , for instance introducing its dependence on the ion size, should improve the obtained results.

To test the reliability of semiempirical predictions, different contributions of the potential energy have been analyzed as a function of the distance of X^- from the center of mass of benzene (r_{X^--bz}). In general, it has been observed that fixing the distance of M^+ from bz at the equilibrium value (V_{M^+-bz} constant), a decrease of r_{X^--bz} originates an increase of V as a consequence of the enhancement of the X^-bz size repulsion. On the other hand, the remaining contributions become less effective (attractive) with an increase of r_{X^--bz} . Concerning the induction energy formulated in this paper from its ion–bond contributions, V'_{ind} and V_{ind} have been analyzed as a function of (r_{X^--bz}) by choosing $Na^+-bz-Cl^-$, for which ab initio results exist,⁴⁵ as a representative example. V'_{ind} and V_{ind} are represented in Figure 4 as a function of r_{Cl^-bz} , where the values of V_{ind} at large distances, different of zero, correspond to the induction energy contribution associated to Na^+-bz . The predicted dependence on r_{Cl^-bz} of V_{ind} agrees with ab initio results.⁴⁵

More interesting is the behavior of the three body term, V'_{ind} , for which it has been also analyzed its peculiar dependence on the aggregate geometry, which is defined from the reference system shown in Figure 5. As can be seen, benzene is placed on the xy plane with the X axis bisecting a CC bond.

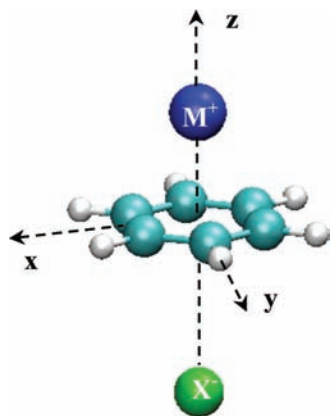


Figure 5. Reference system used to describe the $M^+–bz–X^-$ aggregates.

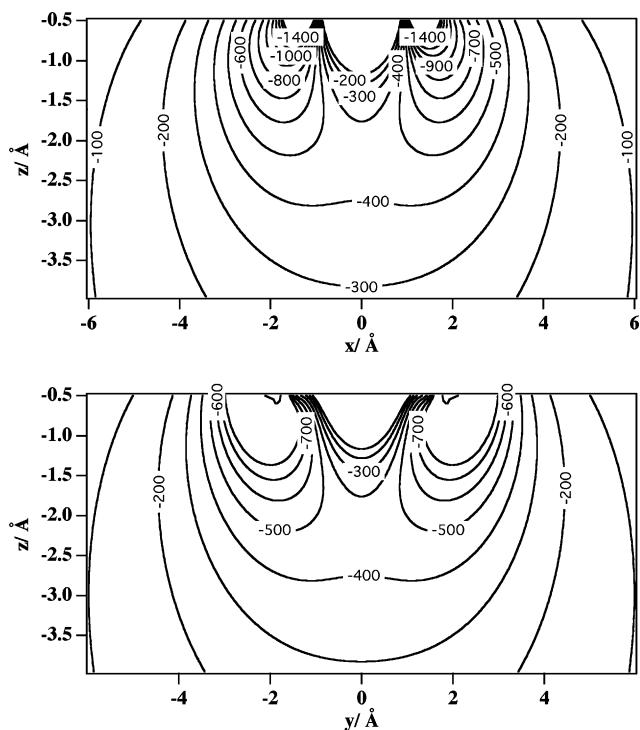


Figure 6. Three body induction energy, V_{ind} , contours (in meV) for the $Na^+–bz–Cl^-$ aggregate with Na^+ fixed along the C_6 axis at $z = 2.154$ Å. Upper panel: Cl^- moves in the xz plane. Lower panel: Cl^- moves in the yz plane (see Figure 5 and text).

Figure 6 reports V_{ind} values for the $Na^+–bz–Cl^-$ aggregate and Cl^- moving, respect to Na^+ , only on the opposite side of bz plane (see Figure 5). It must be stressed that the lowest values of the induction energy (in both the upper and lower panels) are only observed at short distances, which become unaccessible because of the repulsion. Moreover, the adopted function also describes how V_{ind} (not reported in Figure 6) changes when the anion goes from the opposite side of the benzene plane to the same side (respect to the cation).

In this section we have mostly analyzed in detail a peculiar configuration of $M^+–bz–X^-$; however, it is important to note that the proposed methodology provides an analytical function representing the total intermolecular potential V of the system (in all stable and less stable configurations), from which comparisons between different systems can be easily made. This can be appreciated in Figure 7 where equipotential energy contours for the lightest and heaviest aggregates investigated, $Na^+–bz–Cl^-$ (upper panel) and $Cs^+–bz–I^-$ (lower panel), are

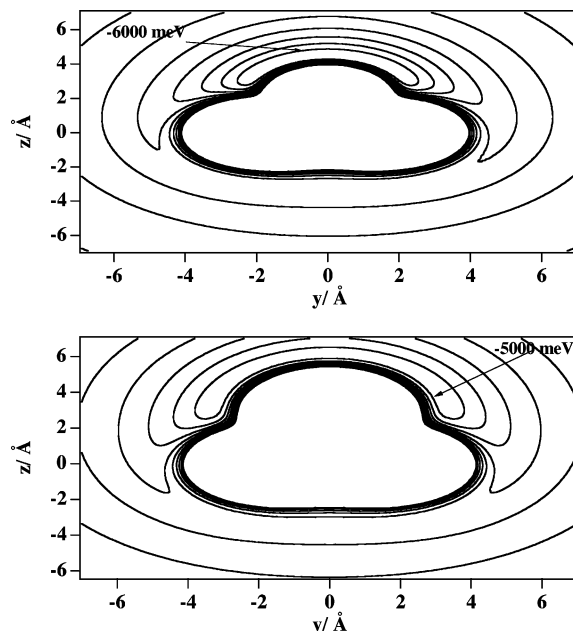


Figure 7. Equipotential energy contours for the $M^+–bz–X^-$ aggregate when X^- moves in the yz plane. Upper panel: $Na^+–bz–Cl^-$ with Na^+ placed at $z = 2.154$ Å. Lower panel: $Cs^+–bz–I^-$ with Cs^+ placed at $z = 2.843$ Å. The lowest energy contours are indicated and consecutive contours are spaced by 500 meV.

shown. The lowest energy contour (associated with the stabler $X^-–M^+–bz$ arrangement) is indicated in each graphic of Figure 7, and consecutive energy contours are spaced by 500 meV. The same figure shows, as indicated before, that the zones with very low (negative) values of the induction energy (see Figure 6) correspond to very repulsive zones of the PES.

4. Conclusions

The main purpose of this study is to demonstrate the effectiveness of the semiempirical method, previously applied to investigate ion– bz aggregates, and how the procedure can be improved and generalized to predict the behavior of systems with increasing complexity. By exploiting the idea that V can be represented as combination of few effective leading components, some of them being expressed as a sum of ion–bond contributions, we have performed a proper assessment of three body induction effects, originated by the presence of a second ion in $M^+–bz–X^-$ systems (with respect to the binary ones). The induction energy has been introduced in such a way that ensures the correct value of the potential energy at all dissociation limits. This is of fundamental importance when applying the PES to perform MD calculations. The potential energy function has been constructed for all $M^+–bz–X^-$ compounds (M = alkali ions and X = halogen ions) except those containing Li^+ and F^- , for which the model is known to be less accurate.^{59,61} Moreover, V has been expressed in a suitable analytical functional form, which allows us to carry out detailed investigations on energy contributions, stable and unstable configurations and on the minimum reaction paths. The simplicity of the potential analytical function should indicate its adequacy to be used to carry out simulations in the context of molecular dynamics. For the investigated systems, the semiempirical approach, without further refinement of the potential parameters, provides for a selected geometry results in good agreement with ab initio calculations and, in general, is able to reproduce most of the ab initio trends.

Acknowledgment. M.A. and A.A. acknowledge financial support from the Ministerio de Educación y Ciencia (Spain, Project CTQ2007-61109). Also thanks are due to the Centre de Supercomputació de Catalunya CESCA-C4 and Fundació Catalana per a la Recerca for the allocated supercomputing time. M.A. also acknowledges financial support from the Ministerio de Ciencia e Innovación (Spain, Mobility Program, Project PR2008-0251). F.P. acknowledges financial support from the Italian Ministry of University and Research (MIUR) for PRIN Contracts.

References and Notes

- Müller-Dethelfs, K.; Hobza, P. *Chem. Rev.* **2000**, *100*, 143.
- Alonso, J. L.; Antolínez, S.; Bianco, S.; Lesarri, A.; López, J. C.; Caminati, W. *J. Am. Chem. Soc.* **2004**, *126*, 3244.
- Aquilanti, V.; Cornicchi, E.; Moix Teixidor, M.; Saendig, N.; Pirani, F.; Cappelletti, D. *Angew. Chem., Int. Ed.* **2005**, *44*, 2336.
- Dykstra, C. E.; Lisy, J. M. *J. Mol. Struct. (THEOCHEM)*. **2000**, *500*, 375.
- Ondrechen, M. J.; Berkovitch-Yellin, Z.; Jortner, J. *J. Am. Chem. Soc.* **1981**, *103*, 6586.
- Fried, L. E.; Mukamel, S. *J. Chem. Phys.* **1991**, *96*, 116.
- Schmidt, M.; Le Calvé, J.; Mons, M. *J. Chem. Phys.* **1993**, *98*, 6102, and references therein.
- Mons, M.; Courty, A.; Schmidt, M.; Le Calvé, J.; Piuze, F.; Dimicoli, I. *J. Chem. Phys.* **1997**, *106*, 1676.
- Easter, D. C.; Bailey, L.; Mellot, J.; Tirres, M.; Weiss, T. *J. Chem. Phys.* **1998**, *108*, 6135.
- Schmidt, M.; Mons, M.; Le Calvé, J. *Chem. Phys. Lett.* **1991**, *177*, 371.
- Brupbacher, Th.; Makarewicz, J.; Bauderm, A. *J. Chem. Phys.* **1994**, *101*, 9736.
- Hobza, P.; Bludsky, O.; Selzle, H. L.; Schlag, E. W. *Chem. Phys. Lett.* **1996**, *250*, 402.
- Lenzer, T.; Luther, K. *J. Chem. Phys.* **1996**, *105*, 10944.
- Bernshtein, V.; Oref, I. *J. Chem. Phys.* **2000**, *112*, 686.
- Vacek, J.; Konvicka, K.; Hobza, P. *Chem. Phys. Lett.* **1994**, *220*, 85.
- Vacek, J.; Hobza, P. *J. Phys. Chem.* **1994**, *98*, 11034.
- Dullweber, A.; Hodges, M. P.; Wales, D. J. *J. Chem. Phys.* **1998**, *106*, 1530.
- Riganelli, A.; Memelli, M.; Laganà, A. *Lect. Notes Comput. Sci.* **2002**, *2331*, 926.
- Zoppi, A.; Becucci, M.; Pietraperzia, G.; Castellucci, E.; Riganelli, A.; Albertí, M.; Memelli, M.; Laganà, A. *Clustering properties of rare gas atoms on aromatic molecules*; 16th International Symposium on Plasma Chemistry, Taormina, Italy, June 2003; p 22.
- Koch, H.; Fernández, B.; Makariewicz, J. *J. Chem. Phys.* **1999**, *111*, 198.
- Cabarcos, O. M.; Weinheimer, C. J.; Lisy, J. M. *J. Chem. Phys.* **1998**, *108*, 5151.
- Cabarcos, O. M.; Weinheimer, C. J.; Lisy, J. M. *J. Chem. Phys.* **1999**, *110*, 8429.
- Dougherty, D. A. *Science* **1996**, *261*, 1708.
- Ma, J. C.; Dougherty, D. A. *Chem. Rev.* **1997**, *97*, 1303.
- Mecozi, S.; West, A. P., Jr.; Dougherty, D. A. *Proc. Natl. Acad. Sci. U.S.A.* **1966**, *93*, 10566.
- Tsuzuki, S.; Yoshida, M.; Uchimarui, T.; Mikami, M. *J. Phys. Chem. A* **2001**, *105*, 769.
- Felder, C.; Jiang, H. L.; Zhu, W. L.; Chen, K. X.; Silman, I.; Botti, S. A.; Sussman, J. L. *J. Phys. Chem. A* **2001**, *105*, 1326.
- Mecozi, S.; West, A. P.; Dougherty, D. A. *J. Am. Chem. Soc.* **1996**, *118*, 2307.
- Cubero, E.; Luque, F. J.; Orozco, M. *Proc. Natl. Acad. Sci. U.S.A.* **1998**, *95*, 5976.
- Caldwell, J. W.; Kollman, P. A. *J. Am. Chem. Soc.* **1995**, *117*, 4177.
- Nicholas, J. B.; Hay, B. P.; Dixon, D. A. *J. Phys. Chem. A* **1999**, *103*, 1394.
- Quiñonero, D.; Garau, C.; Frontera, A.; Ballester, P.; Costa, A.; Deyà, P. M. *J. Phys. Chem. A* **2005**, *109*, 4632.
- Jalbout, A. F.; Adamowicz, L. *J. Chem. Phys.* **2002**, *116*, 9672.
- Morais-Cabral, J. H.; Zhou, Y.; MacKinnon, R. *Nature* **2001**, *414*, 37.
- Kumpf, R. A.; Dougherty, D. A. *Science* **1993**, *271*, 163.
- Lehn, J. M. *Supramolecular Chemistry*; VCH: Weinheim, 1995.
- Meyer, E. A.; Castellano, R. K.; Diederich, F. *Angew. Chem. Int. Ed.* **2003**, *42*, 1210.
- Bianchi, G. P.; Wayner, D. D. M.; Wolkow, R. A. *Nature* **2000**, *406*, 48.
- Gallivan, J. P.; Dougherty, D. A. *Proc. Natl. Acad. Sci. U.S.A.* **1999**, *96*, 9459.
- Schottel, B. L.; Chifotides, H. T.; Dunbar, K. R. *Chem. Soc. Rev.* **2008**, *37*, 68.
- Gokel, G. W.; Barbour, L. J.; De Wall, S. L.; Meadows, E. S. *Coord. Chem. Rev.* **2001**, *222*, 127.
- Feller, D.; Dixon, D. A.; Nicholas, J. B. *J. Phys. Chem. A* **2000**, *104*, 11414.
- Coletti, C.; Re, N. *J. Phys. Chem. A* **2006**, *110*, 6563.
- Reddy, A. S.; Sastry, G. N. *J. Phys. Chem. A* **2005**, *109*, 8893.
- Kim, D.; Lee, E. C. X.; Kim, K. S.; Tarakeshwar, P. *J. Phys. Chem. A* **2007**, *111*, 7980.
- Bianchi, A.; Bowman-James, K.; García-España, E., Eds. *Supramolecular Chemistry of Anions*; Wiley: New York, 1997.
- Imai, Y. N.; Inoue, Y.; Nakanishi, I.; Kitauro, K. *Protein Sci.* **2008**, *17*, 1129.
- (a) Li, Y.; Flood, A. H. *J. Am. Chem. Soc.* **2008**, *130*, 12111. (b) Alcalde, E.; Mesquida, N.; Vilaseca, M.; Alvarez-Rúa, C.; García-Granda, S. *Supramol. Chem.* **2007**, *19*, 501.
- Cerichelli, G.; Mancini, G. *Langmuir* **2000**, *16*, 182.
- Mascal, M.; Armstrong, A.; Bartberger, M. D. *J. Am. Chem. Soc.* **2002**, *124*, 6274.
- Schneider, H.; Vogelhuber, K. M.; Shinle, F.; Weber, J. M. *J. Am. Chem. Soc.* **2007**, *129*, 13022.
- Garau, C.; Frontera, A.; Quiñonero, D.; Ballester, P.; Costa, A.; Deyà, P. M. *Chem. Phys. Chem.* **2003**, *4*, 1344.
- Garau, C.; Quiñonero, D.; Frontera, A.; Costa, A.; Ballester, P.; Deyà, P. M. *Chem. Phys. Lett.* **2003**, *370*, 7.
- Beer, P. D.; Galle, P. A. *Angew. Chem. Int. Ed.* **2001**, *40*, 486.
- Pirani, F.; Albertí, M.; Castro, A.; Moix, M.; Cappelletti, D. *Chem. Phys. Lett.* **2004**, *394*, 37.
- Pirani, P.; Brizi, S.; Roncaratti, L. F.; Casavecchia, P.; Cappelletti, D.; Vecchiocattivi, F. *Phys. Chem. Chem. Phys.* **2008**, *10*, 5489.
- Pirani, F.; Cappelletti, D.; Liuti, G. *Chem. Phys. Lett.* **2001**, *350*, 286.
- Albertí, M.; Castro, A.; Laganà, A.; Moix, M.; Pirani, F.; Cappelletti, D.; Liuti, G. *J. Phys. Chem. A* **2005**, *110*, 9002.
- Albertí, M.; Aguilar, A.; Lucas, J. M.; Pirani, F.; Cappelletti, D.; Coletti, C.; Re, N. *J. Phys. Chem. A* **2006**, *109*, 2906.
- Coletti, C.; Re, N. *J. Phys. Chem. A* **2009**, *113*, 1578.
- Albertí, M.; Aguilar, A.; Lucas, J. M.; Pirani, F.; Coletti, C.; Re, N. *J. Phys. Chem. A*, DOI: 10.1021/jp9043295.
- Albertí, M.; Aguilar, A.; Lucas, J. M.; Laganà, A.; Pirani, F. *J. Phys. Chem. A* **2007**, *111*, 1780.
- Huarte-Larragaña, F.; Aguilar, A.; Lucas, J. M.; Albertí, M. *J. Phys. Chem. A* **2007**, *111*, 8072.
- Albertí, M.; Aguilar, A.; Lucas, J. M.; Cappelletti, D.; Laganà, A.; Pirani, F. *Chem. Phys. Chem.* **2006**, *328*, 221.
- Albertí, M.; Castro, A.; Laganà, A.; Moix, M.; Pirani, F.; Cappelletti, D. *Eur. Phys. J. D* **2006**, *38*, 185.
- Albertí, M.; Aguilar, A.; Lucas, J. M.; Pirani, F. *Theor. Chem. Acc.* **2009**, *123*, 21.
- MacGillivray, L. R.; Atwood, J. L. *J. Chem. Soc., Chem. Commun.* **1997**, 477.
- Izatt, R. M.; Pawlak, K.; Bradshaw, J. S.; Bruening, R. L. *Chem. Rev.* **1991**, *91*, 1721.
- Izatt, R. M.; Pawlak, K.; Bradshaw, J. S.; Bruening, R. L. *Chem. Rev.* **1995**, *95*, 2529.
- Islam, M. S.; Pethrick, R. A.; Pugh, D.; Wilsom, M. J. *J. Chem. Soc., Faraday Trans.* **1998**, *94*, 39.
- Nathanson, G. M.; Davidovits, P.; Workshop, D. R.; Kolb, C. E. *J. Phys. Chem.* **1996**, *100*, 13007.
- Laskin, A.; Gaspar, D. J.; Wang, W.; Hunt, S. W.; Cowin, J. P.; Colson, S. D.; Finlayson-Pitts, B. J. *Science* **2003**, *301*, 340.
- Albertí, M.; Castro, A.; Laganà, A.; Pirani, F.; Porrini, M.; Cappelletti, D. *Chem. Phys. Lett.* **2004**, *392*, 514.
- Aquilanti, V.; Cappelletti, D.; Pirani, F. *Chem. Phys.* **1996**, *209*, 299.
- http://www.cse.clrc.ac.uk/ccg/software/DL_POLY/index.shtml.